J Polym Environ (2017) 25:229–240
DOI 10.1007/s10924-016-0801-8

ORIGINAL PAPER

Toughening of Polyvinyl Alcohol Hydrogel Through Co-Crosslinking and its Wastewater Treatment Performance by Immobilizing with Microorganism

Ge Zhang[1] · Lin Ye[1]

Published online: 5 August 2016

Abstract In order to improve the hydraulic impact resistance of the polyvinyl alcohol (PVA) hydrogel as microorganism immobilization carrier and meet the requirements of long-time aeration of sewage treatment, the toughening PVA hydrogel beads were prepared by co-crosslinking with polyoxypropylene triol (PPG) through the boric acid (H_3BO_3)-chemical crosslinking method. It was found that PPG could increase the consumption of H_3BO_3, participated and accelerated the crosslinking reaction of PVA, and the pore size of the surface layer and core layer of the hydrogel beads can be controlled. With increasing PPG content, the shear storage modulus (G') and the effective network density (ν_e) increased first, reached maximum in presence of 2 wt% PPG, and decreased afterwards. A relatively low content of PPG could promote the formation of relatively uniform and dense network structure in PVA hydrogel, resulting in an improvement of the mechanical property and long-term hydraulic stability of the gel beads. By addition of PPG, the capillary water absorption capacity of PVA hydrogel can be enhanced and the high permeability can be kept well. When applying in waste water treatment, the value of the oxygen uptake rate (OUR) and COD removal rate of the PVA hydrogel immobilized with activated sludge had no obvious difference with addition of PPG, and a high microbial activity can be maintained.

✉ Lin Ye
yelinwh@126.com

[1] State Key Laboratory of Polymer Materials Engineering, Polymer Research Institute of Sichuan University, Chengdu 610065, China

Keywords Polyvinyl alcohol (PVA) hydrogel · Co-crosslinking · Crosslinking network structure · Toughening mechanism · Microbial activity

Introduction

Water pollution is well acknowledged to be harmful to the majority of living organisms, and has become one of the serious environmental problems of worldwide concern. Immobilization of microbial cells has received increasing interest in the field of waste water treatment [1–7]. It not only offers a high cell concentration in the reaction tank for increasing biodegradation efficiency, but also it is advantageous for the separation of liquid and solid in the settling tank.

Crosslinked poly(vinyl alcohol) (PVA) hydrogels are hydrophilic three-dimensional polymeric networks, which are insoluble in water due to the presence of chemical or physical crosslinks. They have good biocompatibility, non-toxicity, high elastic modulus and low cost, attracting great attention in microorganism immobilization for waste water treatment [8–15]. However, in sewage aeration tank, the strong shear force produced by oxygen aeration and fluid turbulence made the hydrogel beads easy to be broken and damaged, which required them to possess high hydraulic impact resistance, in order to meet the requirements of long-time running of sewage treatment [16]. Few literatures on the improvement of the mechanical toughness of PVA hydrogels can be available. Sirousazar etc. used mineral kaolinite clay to modify PVA hydrogels through freezing/thawing cyclic method, resulting in an improvement of mechanical property of PVA matrix [17]. Jianyu Li etc. prepared PVA- polyacrylamide hydrogel consisting of a hydrophilic polyacrylamide network that was covalently

cross-linked and a PVA network that formed crystallites, which combined extremely high stiffness, strength, and toughness [18].

For PVA hydrogel beads crosslinked by boric acid (H_3BO_3) [19–22], their surfaces crosslinked rapidly when contacting with the curing agent solution. The formed dense crosslinked shell may hinder the curing agent solution to further disperse into core layer of the hydrogel, resulting in the low crosslinking degree and loose structure of the core layer. And thus the un-uniform crosslinking porous structure formed, leading to low mechanical strength of PVA hydrogel beads.

Polyoxypropylene triol (PPG) is a tri-arm oligomer with long flexible chains consisting of ether bonds and three terminal primary hydroxyls. And the primary hydroxyl groups are more reactive than the secondary hydroxyl group on PVA molecular chains. Therefore in this work, through the competition reaction of PPG and PVA with H_3BO_3, the crosslinking reaction rate of the surface layer and core layer of the PVA hydrogel beads was expected to be controlled for the formation of the homogeneous crosslinking network structure. Moreover, by introduction of the flexible polyether chains of PPG onto the PVA molecular chains, the mechanical toughness of the hydrogel can be expected to be improved. The effect of PPG on the crosslinking reactive kinetics and the network structure of PVA was studied, and the toughening mechanism was explored. The permeability and swelling behavior were discussed. Furthermore, the PVA hydrogel was applied in the waste water treatment by immobilizing with microorganism, and the properties of hydraulic impact resistance and waste water treatment efficiency were investigated.

Experimental

Materials

PVA with an average molecular weight (M_n) of 74,800 g/mol was supplied by Sichuan Vinylon Co. (China). Sodium alginate (Alg) was purchased from Kelong Chemical Co. (Chengdu, China). Boric acid (H_3BO_3) and PPG with an average molecular weight (M_n) of 3000 g/mol were purchased from Bodi Chemical Co. (Tianjin, China). Other chemical agents were all of analytical purity and used as received. The wastewater and activated sludge were collected from Chengdu Drainage Co. (Chengdu, China) on the day for preparation of PVA hydrogel beads.

Preparation of PVA Hydrogel Beads

PVA (10 g), Alg (1 g) and PPG (0–0.4 g) were dissolved in the distilled water (100 ml) by magnetic stirring at 95 °C. The mixture was cooled to room temperature and dropped into the saturated H_3BO_3 and $CaCl_2$ solution, keeping for 1 h to form spherical beads. The formed beads were finally soaked and washed with distilled water, and stored in distilled water at room temperature. The diameter of hydrogel beads ranged from 4 to 6 mm. For preparation of PVA hydrogel beads immobilized with microorganisms, the sludge (10 g) was added after the PVA/Alg/PPG mixture was cooled to room temperature.

Measurements

H_3BO_3 Concentration

Boric acid was extremely weak acid, and its concentration can't be determined directly with alkali titration. In order to enhance acidity of boric acid, mannitol is added to the aqueous solution of boric acid to generate a complex acid, which concentration could be measured directly through alkali standard solution titration.

Specific operation was as follows: for the crosslinking reaction system of PVA/PPG/H_3BO_3, 1 ml reaction solution was taken out and added to 25.0 ml distilled water, then 2.5–3.0 g mannitol was added. After well mixed, 1 % phenolphthalein indicator was added and titrated with 0.1 mol/L NaOH standard solution. The H_3BO_3 concentration can thus be calculated with the consumption of NaOH standard solution.

Fourier Transform Infrared (FTIR) Analysis

The samples of PVA hydrogel were first dried and analyzed with a Nicolet-560 FTIR spectrometer (Madison of WO, USA). The pellet sample was prepared by pressing the mixture of the PVA samples and KBr powder. The scanning rate is 20 min^{-1}, and the differentiate rate is 4 cm^{-1}.

Mechanical Property

The tensile property of the samples of PVA hydrogel was measured with a 4302 material testing machine from Instron Co. (USA) according to GB/T 528-1998. The tensile speed and temperature were 50 mm/min and 23 °C, respectively.

The hydraulic impact property of PVA hydrogel can be measured as follows: PVA hydrogel beads were put into the distilled water, stirring at room temperature with stirring speed 2000 r/min. The retention rate of gel beads without damage as a function of time was calculated with the following equation:

$$\textit{Retention rate}\,(\%) = N_t/N_0 \times 100\,\% \qquad (2.1)$$

where N_0 was initial number of gel beads; N_t was the number of gel beads at time t.

Rheological Property

The viscoelasticity properties of PVA hydrogel were measured on Rheometer System Gemini 200 of Malvern Instrument Co. (UK) with parallel plates with diameter of 25 mm and a plate-to-plate distance of 1–2 mm. Both the strain and the frequency sweep experiments were performed at room temperature. In strain sweep measurements, the shear storage modulus (G') and loss modulus (G'') were recorded at the strain of 0.005–10 % and the frequency of 1 Hz. In the frequency sweep experiments, G' and G'' were measured in the linear viscoelastic regime, for frequencies ranging from 0.1 to 100 Hz, at a maximum strain, γ, of 0.1 %. This γ value was determined by preliminary strain sweep experiments, in which G' and G'' were measured as a function of strain at a fixed frequency value of 1 Hz to check if the deformation imposed on the gel structure during the rheological experiment was entirely reversible.

Swelling Ratio

The pre-weighed dry samples of PVA hydrogel were immersed into the distilled water at room temperature until they swelled to equilibrium. After excessive surface water was removed with filter paper, the samples were weighed. The swelling ratio can be determined as a function of time [23, 24]:

$$Swelling\ ratio\,(\%) = (W_t - W_0)/W_0 \times 100\,\% \qquad (2.2)$$

where W_0 was the dried weight of hydrogel, and W_t was the weight of hydrogel in swollen state at time t.

Permeability of PVA Hydrogel

PVA gel beads were immersed into the diluted ink, and kept for 3 hours at room temperature. The UV transmission rate of ink solution at band 450–700 nm was measured with U3010 UV–visible spectrophotometer (Japan), which was used to characterize the permeability of the gel beads.

Scanning Electron Microscope (SEM) Analysis

The fractured surface morphology of PVA hydrogel beads was observed with a JEOL JSM-5900LV SEM (Japan) with an acceleration voltage of 20 kV. The PVA hydrogel beads were freezing dried and cryogenically fractured in liquid nitrogen. Then the samples were sputter-coated with gold for 2–3 min.

Oxygen Uptake Rate (OUR)

About 100 ml distilled water was put into a flask, and aerated to make the dissolved oxygen saturated by air pump. Stop aeration and 5 g of PVA hydrogel beads immobilized with sludge was added. The concentration of the dissolved oxygen (DO) variation with time was measured with AZ 8403 DO meter (China), and the OUR value can be calculated with the following equation [25, 26]:

$$OUR = \frac{DO_1 - DO_2}{t_2 - t_1} \quad t = t_2 - t_1 \qquad (2.3)$$

where DO_1 was the concentration of the dissolved oxygen at time t_1; DO_2 was the concentration of the dissolved oxygen at time t_2; t was the measuring time.

Chemical Oxygen Demand (COD) removal rate

COD value of the wastewater mainly depends on the composition and concentration of organic contaminants, and the absorbance of the organics has good correlation with COD. The wastewater solution with different concentrations was prepared, the UV absorbance of the solution at 254 nm was measured with U3010 UV–visible spectrophotometer (Japan), and the standard curve of UV absorbance-wastewater concentration was obtained.

The absorbance at 254 nm of the sample was measured, and the corresponding wastewater concentration can be obtained by the standard curve [27–29]. The COD removal rate was then calculated with the following equation:

$$COD\ removal\ rate\ (\%) = (C_t - C_0)/C_t \times 100\,\% \qquad (2.4)$$

where C_0 was the original wastewater concentration before treatment, and C_t was the wastewater concentration after treatment.

Results and Discussion

Effect of PPG on the Crosslinking Reaction Kinetics of PVA Hydrogel

During the crosslinking reaction of PVA/PPG system by using H_3BO_3 as the crosslinking agent, both the hydroxyl groups on the molecular chain of PVA and PPG could react with H_3BO_3. Therefore, the effect of PPG on the crosslinking reaction kinetics of PVA hydrogel was investigated. Figure 1 illustrated the molar concentration of H_3BO_3 versus crosslinking time of PVA hydrolgels with different content of PPG. It can be seen that during the first 20 min of reaction, the molar concentration of H_3BO_3 decreased sharply, and reached equilibrium in about

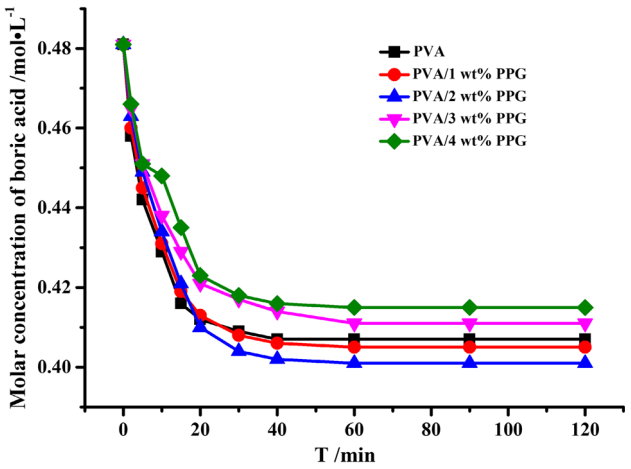

Fig. 1 The molar concentration of H_3BO_3 versus crosslinking time of PVA/PPG system

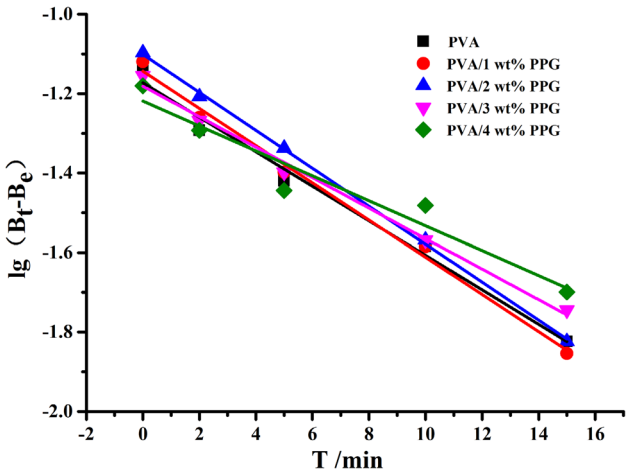

Fig. 2 Crosslinking reaction kinetics of PVA/PPG system

60 min. With increasing content of PPG, the molar equilibrium concentration of H_3BO_3 decreased first, reached minimum in presence of 2 wt% PPG, and increased afterwards, indicating that PPG could increase the consumption of H_3BO_3 and participate the crosslinking reaction of PVA.

The crosslinking reaction kinetics of PVA composite hydrogel was analyzed by assuming that the crosslinking reaction process met the first order kinetic equation:

$$dB_t/dt = -k(B_t - B_e) \tag{3.1}$$

where t was crosslinking reaction time; B_t, molar concentration of boric acid at time t; B_e, molar concentration of H_3BO_3 when crosslinking reaction reached the equilibrium; dB_t/dt, crosslinking reaction rate; and k, the crosslinking reaction rate constant. The crosslinking reaction equation can be obtained by integral of the above equation:

$$B_t = B_e + (B_0 - B_e)/e^{kt} \tag{3.2}$$

Another form of the equation can be written as:

$$lg(B_t - B_e) = -kt/2.303 + lg(B_o - B_e) \tag{3.3}$$

By plotting the graph of $lg\ (B_t - B_e)$ versus time t, as shown in Fig. 2, the crosslinking reaction rate constant k can be obtained from the slope of the curve, which exhibited good linear relationship.

As listed in Table 1, it can be seen that with increasing content of PPG, the crosslinking reaction rate constant k of PVA hydrogel increased first, reached maximum in presence of 2 wt% PPG, and decreased afterwards, indicating that low content of PPG accelerated the crosslinking reaction.

For PVA in absence of PPG, the crosslinking reaction of PVA with H_3BO_3 started on the surface layer of the liquid drops of PVA solution and the formed dense crosslinking networks may hinder H_3BO_3 to penetrate into core layer of PVA liquid drops, resulting in a relatively low crosslinking degree and inhomogeneous network structure.

For PVA in presence of PPG, because the primary hydroxyl groups of PPG were more reactive than the secondary hydroxyl group on PVA molecular chains, the crosslinking reaction rate of the former was higher than that of the latter, and the crosslinking reaction of PVA on the surface of the hydrogel can be slowed down. Thus H_3BO_3 and the formed PPG-borate could percolate into the core of the drops, which promoted the crosslinking reaction of PVA in the core layer, leading to the increase of the consumption of H_3BO_3 and the crosslinking reaction rate of the whole system. However, the amount of hydroxyl groups within PPG is much less than that of hydroxyl groups on PVA molecular chains, so under excessive addition of PPG, the consumption of H_3BO_3 and the crosslinking reaction rate decreased.

The observation of the internal morphology of PVA hydrogel and PVA/PPG hydrogel was carried out. Figure 3 showed SEM images of the cross section of PVA hydrogel and PVA/2 wt%PPG hydrogel. It can be seen that, for PVA hydrogel, the morphology of core layer and surface layer had obvious differences: the pores were dense and small on the surface layer, whereas the pores were loose and large in the core layer. However, for PVA/2 wt%PPG hydrogel, the pores of core layer and surface layer of exhibited similar size with relatively uniform structure.

The pore size distribution for the PVA hydrogel and PVA/PPG hydrogel were summarized in Fig. 4. It can be clearly observed that for PVA hydrogel, the diameter of pore on the surface layer ranged from 0 to 6 μm, and focused on 0–4 μm. The pore size distribution of core layer ranged from 0 to 14 μm, and focused on 0–6 μm. However, for PVA/PPG hydrogel, the pore on the surface layer had larger and uniform size, and the diameter of pore

Table 1 Crosslinking reaction rate constant of PVA/PPG system

Sample	Reaction rate constant k (h^{-1})	Equilibrium H_3BO_3 molar concentration (mol L^{-1})
PVA	6.00	0.407
PVA/1 wt% PPG	6.47	0.405
PVA/2 wt% PPG	6.60	0.401
PVA/3 wt% PPG	5.27	0.403
PVA/4 wt% PPG	4.33	0.404

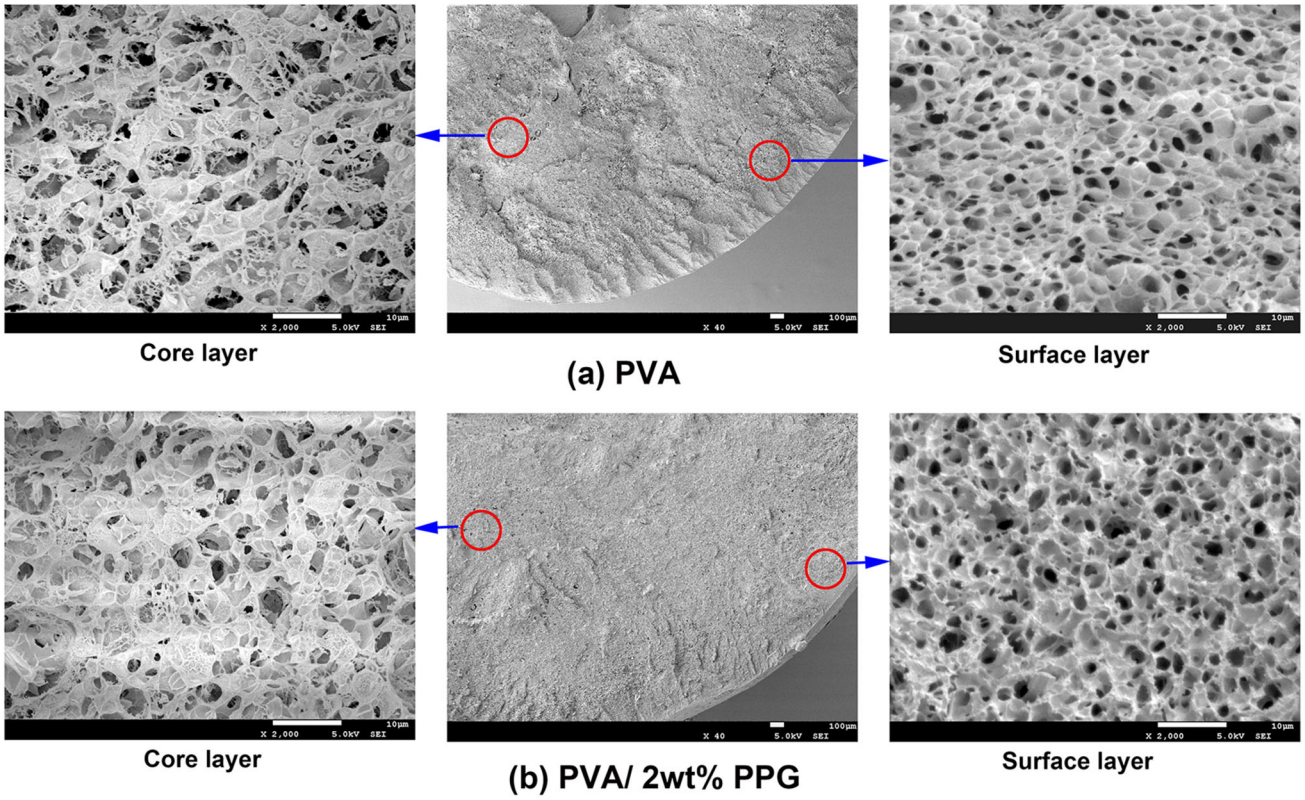

Fig. 3 SEM image of the cross section of PVA hydrogel and PVA/2 wt% PPG hydrogel (Magnification: ×2000)

ranged from 0 to 6 μm, and focused on 2–4 μm. Meanwhile, the pore size distribution of core layer ranged from 0 to 10 μm, and focused on 2–6 μm. This indicated that introduction of PPG could control pore size of surface layer and core layer of PVA hydrogel beads, and make the porous structure more uniform.

The FT-IR spectra of PPG, PVA hydrogel and PVA/PPG hydrogel were shown in Fig. 5. The pure PPG sample showed a characteristic band at 1109 cm^{-1}, attributed to the irregular C–O–C stretching vibration. The characteristic bands at 2972 and 2870 cm^{-1} were attributed to dissymmetrical stretching and symmetrical stretching vibration of $–CH_3$, and the characteristic band at 3483 cm^{-1} was attributed to the terminal –OH stretching absorption [30]. For the sample of PVA hydrogel, a wide absorption band at 3458 cm^{-1} was attributed to the presence of –OH [31, 32]. The absorption band at 2924 cm^{-1} was attributed to dissymmetrical stretching vibration of $–CH_2$. The absorption band at 1067 cm^{-1} was attributed to the presence of C-O bond, and the absorption band at 877 cm^{-1} was attributed to stretching vibration of C–C bond [33]. For the sample of PVA/PPG hydrogel, the absorption band of C–O at 1067 cm^{-1} became stronger compared with the pure PVA sample. And the absorption peak of hydroxyl groups blue shifted from 3458 cm^{-1} of the pure PVA sample toward higher wave number at about 3486 cm^{-1}, due to the weakened intramolecular hydrogen bonding of PVA by incorporation of PPG.

Based on the above analysis results, the crosslinking reaction and intermolecular bonding of PVA/PPG hydrogel system can be deduced, including the crosslinking reaction of PVA with H_3BO_3, the crosslinking reaction of PPG with

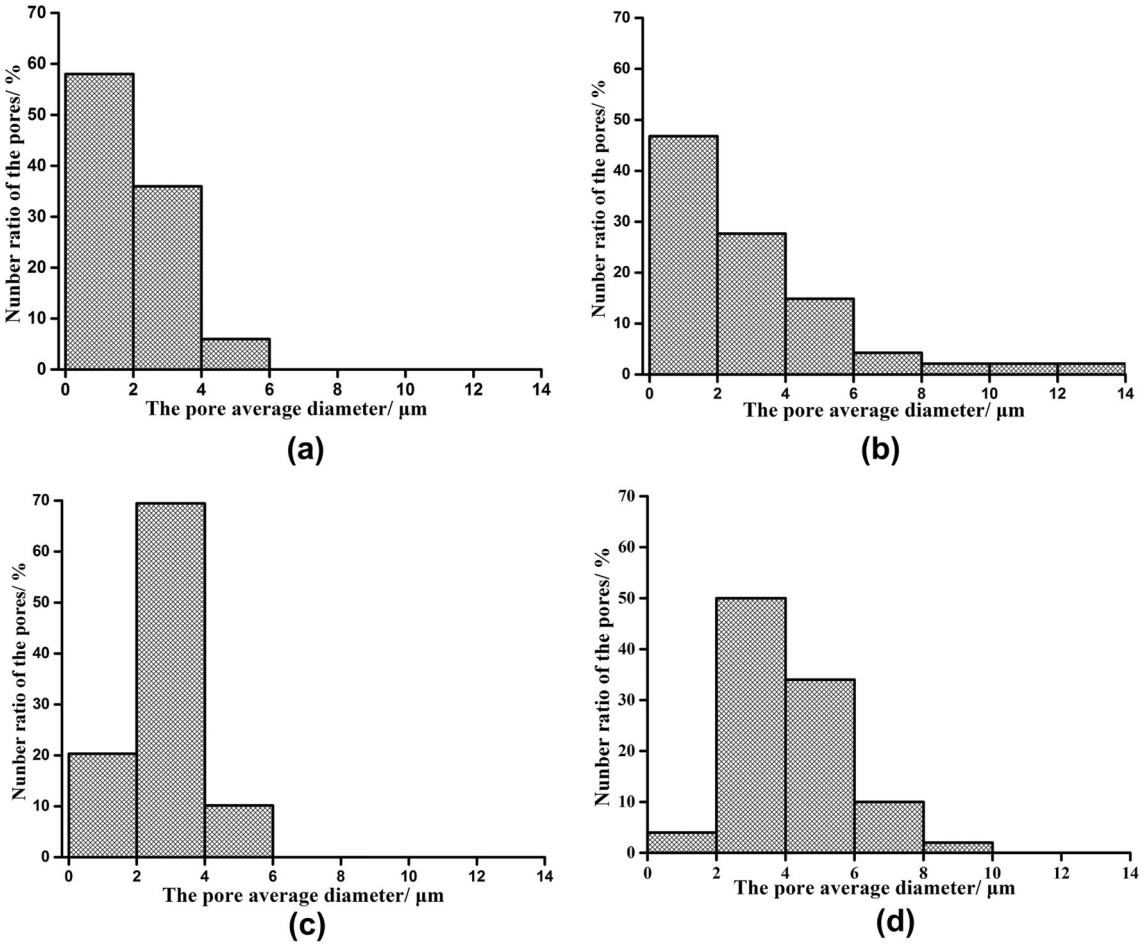

Fig. 4 Pore size distribution of PVA hydrogel and PVA/2 wt% PPG hydrogel. **a** Surface layer of PVA hydrogel. **b** Core layer of the PVA hydrogel. **c** Surface layer of PVA/2 wt% PPG hydrogel. **d** Core layer of the PVA/2 wt% PPG hydrogel

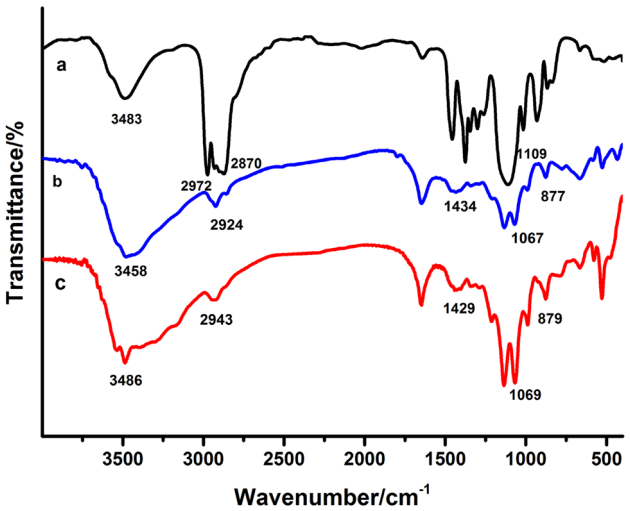

Fig. 5 FTIR spectra of **a** PPG **b** PVA **c** PVA/2 wt% PPG hydrogel

H_3BO_3, the co-crosslinking reaction of PPG/PVA with H_3BO_3, which introduced PPG into PVA crosslinking network, as shown in Fig. 6.

Effect of PPG on the Crosslinking Network Structure of PVA Hydrogel

Figure 7 showed the strain dependence of the shear storage modulus (G') and loss modulus (G'') at the frequency of 1 Hz for PVA hydrogel with different content of PPG. At very low strain amplitudes, the loss modulus of the hydrogel was lower than the storage modulus, which was consistent with the existence of a network structure. In addition, it can be noted that, for small strain amplitudes, G' was independent of the strain amplitude, which indicated that the deformation imposed on the network structure was entirely reversible. At higher strain amplitudes, G' was a decreasing function of the strain amplitude and the deformation was no longer reversible.

The frequency dependence of G' was plotted in Fig. 8 for PVA hydrogel with different content of PPG. It can be seen that G' did not depend on the test frequency in the range between 0.1 and 100 Hz for all samples, indicating that the elastic behavior of these samples predominated

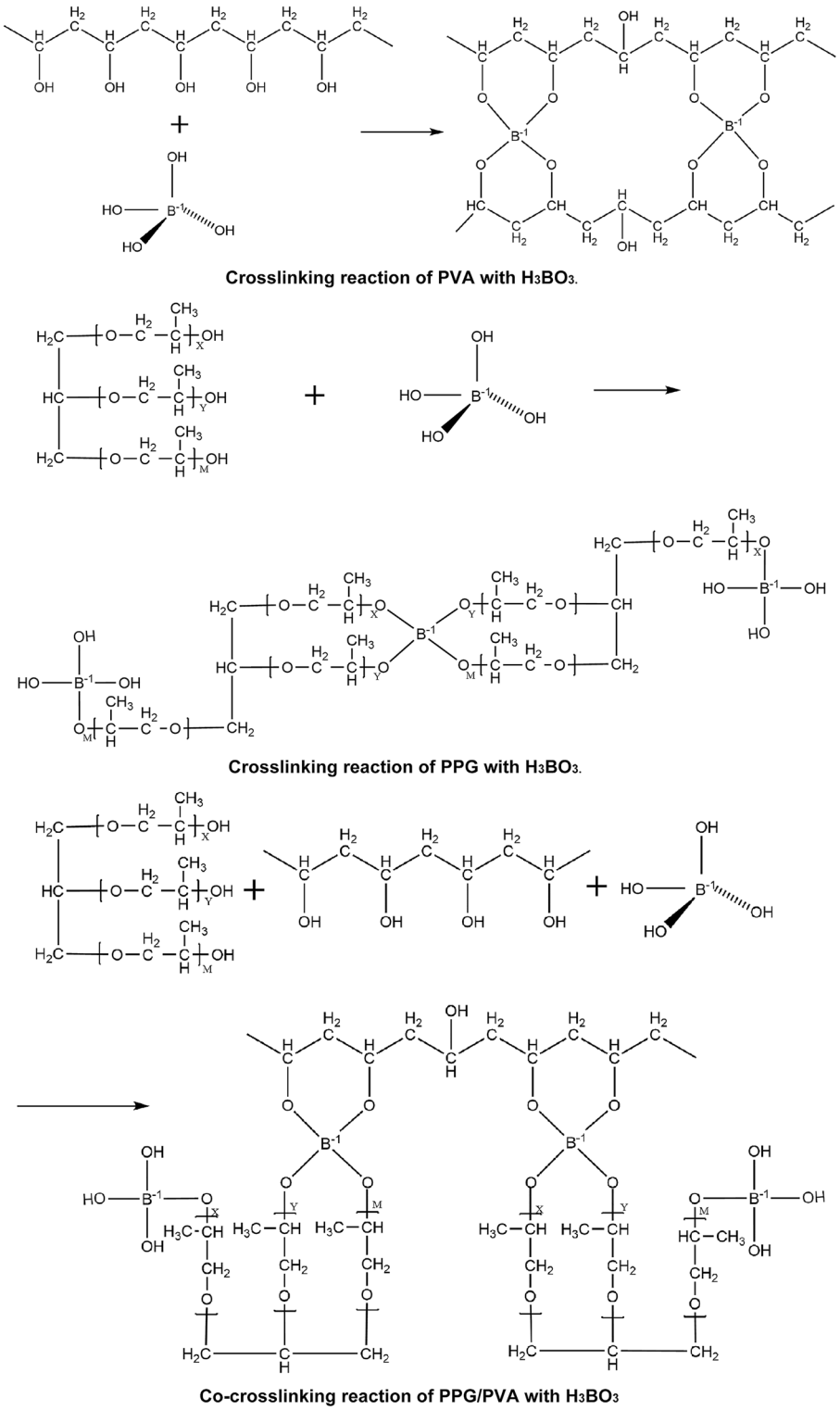

Fig. 6 Schematic representation of the crosslinking reaction and intermolecular bonding of PVA/PPG system

over their viscous behavior, and a perfect network formed. With increasing content of PPG, G' increased first, reached maximum in presence of 2 wt% PPG, and decreased afterwards. A relatively low content of PPG could increase the consumption of H_3BO_3 and crosslinking density of the whole system. In addition, the association of the long flexible polyether chains of PPG led to the intermolecular physical entanglement. However, excessive addition of PPG decreased the consumption of H_3BO_3 and crosslinking density of the whole system.

Equilibrium water content (EWC), the volume fraction of polymer in the hydrogel at equilibrium swelling, Φ_1, and

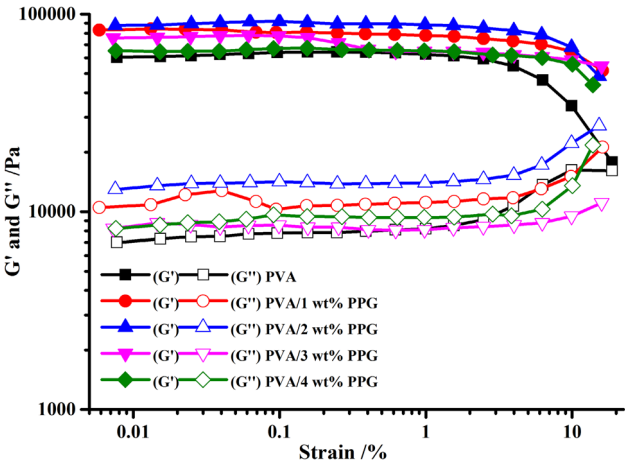

Fig. 7 Strain dependence of G' and G'' for PVA hydrogel with various PPG content

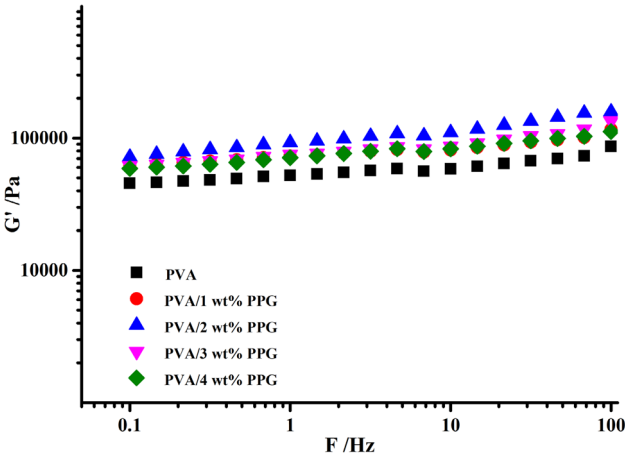

Fig. 8 Frequency dependence of G' for PVA hydrogel with various PPG content

the volume fraction of the crosslinking polymer in the relaxed state, Φ_2, can be calculated as follows [34, 35]:

$$ECW\ (\%) = \frac{W_e - W_d}{W_e} \times 100 \tag{3.4}$$

$$\phi_1 = \frac{W_d/\rho_p}{W_d/\rho_p + (W_e - W_d)/\rho_s} \tag{3.5}$$

$$\phi_2 = \frac{W_d/\rho_p}{W_d/\rho_p + (W_r - W_d)/\rho_s} \tag{3.6}$$

where W_d was the weight of the dry gel, W_r was the weight of the relaxed gel and W_e was the weight of gel at the equilibrium swollen state, and ρ_p and ρ_s were the densities of polymer and water, respectively. The density of the PVA matrix (ρ_p) was 1.388 g/cm^3.

The effective network density (ν_e) of the PVA hydrogel was determined from the following equation based on the rubber elasticity theory:

$$G = RT\nu_e\phi_1^{1/3}\phi_2^{2/3} \tag{3.7}$$

where R was the gas constant, T was the temperature. The average molecular mass between crosslinks, M_c, was calculated as follows:

$$M_c = \frac{\rho_p}{\nu_e}. \tag{3.8}$$

The value of G', ν_e and M_c of PVA hydrogel with different content of PPG were calculated and listed in Table 2. It can be seen that, with increasing PPG content, G' and ν_e increased first, reached maximum in presence of 2 wt% PPG where M_c reached minimum, and decreased afterwards, indicating that a relatively low content of PPG could promote the formation of relatively uniform and dense network structure in PVA hydrogel due to the acceleration effect of PPG on the crosslinking reaction of PVA system, and the association of its long flexible polyether chains. Excessive addition of PPG led to the retarding of PVA crosslinking reaction and decrease of crosslinking density of the whole system.

Effect of PPG on the Mechanical Properties of PVA Hydrogel

Table 3 showed the effect of PPG content on the hydraulic impact resistance of PVA hydrogel beads. It can be seen that after 4 h' hydraulic impact test, the pure PVA hydrogel beads were completely destroyed. By addition of PPG, the crushing strength of the hydrogel beads was dramatically improved. With increasing content of PPG, the retention rate of gel beads increased first, reached the maximum at 2 wt% PPG, and then decreased. It took about 12 h for PVA/2 wt% PPG gel beads to be completely destroyed. These results indicated that proper content of PPG could toughen and strengthen PVA hydrogel.

The mechanical property of PVA hydrogel with varying content of PPG was depicted in Fig. 9. It can be seen that with increasing content of PPG, the tensile strength of PVA hydrogel increased dramatically, reached maximum with the addition of 2 wt% PPG, and decreased afterwards. The maximum tensile strength of PVA/2 wt% PPG hydrogel increased by 50 %. The elongation at break of the hydrogel fluctuated slightly within the investigated range of PPG content.

Furthermore, the long-term hydraulic stability of PVA/2 wt% PPG hydrogel beads immobilized with microorganism in the process of wastewater treatment was investigated. Figure 10 showed photos of the hydrogel samples before and after long-term aeration. It can be seen that after 10 months aeration test, the surface of the hydrogel beads was not damaged, and the shape and size of the beads were kept well, indicating that PVA/PPG hydrogel immobilized with microorganism had excellent long-term hydraulic stability.

Table 2 Network parameters of PVA hydrogel with various PPG content

Sample	ρ_p (g/cm^3)	Φ_1	Φ_2	G' (KPa)	ν_e (mol/m^3)	M_c (kg/mol)
PVA	1.388	0.1576	1	52.3	38.44	36.11
PVA/1 wt% PPG	1.384	0.1254	1	73.2	58.05	23.84
PVA/2 wt% PPG	1.381	0.1231	1	92.4	73.73	18.73
PVA/3 wt% PPG	1.378	0.1156	1	75.0	61.26	22.49
PVA/4 wt% PPG	1.375	0.1094	1	71.1	59.01	23.30

Table 3 Crushing strength of PVA hydrogel beads with various PPG content

Sample	Time (h)								
	Retention rate (%)								
	4	5	6	7	8	9	10	11	12
PVA	60	0	0	0	0	0	0	0	0
PVA/1 wt% PPG	100	100	68	28	0	0	0	0	0
PVA/2 wt% PPG	100	100	100	100	100	80	64	36	0
PVA/3 wt% PPG	100	100	100	64	32	0	0	0	0
PVA/4 wt% PPG	100	72	30	0	0	0	0	0	0

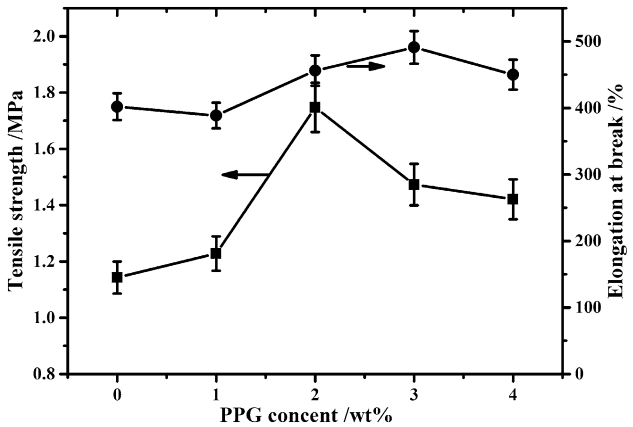

Fig. 9 Mechanical properties of PVA hydrogel with various PPG content

Based on the above discussion, the toughening mechanism of PVA/PPG hydrogel was deduced: PPG as a tri-arm oligomer with polyether chains and three terminal hydroxyls was incorporated into the crosslinking network of PVA by reacting with H_3BO_3. Introduction of PPG changed the crosslinking reaction pathway of PVA by slowing down the crosslinking reaction of the surface layer of the liquid drop of PVA solution and promoting the crosslinking reaction in its core layer, resulting in the formation of more regular and uniform porous structure of the hydrogel. In addition, the introduced long flexible polyether chains of PPG and the increasing effective network density resulted in an improvement of mechanical strength and toughness, and the hydraulic impact resistance of PVA hydrogel beads.

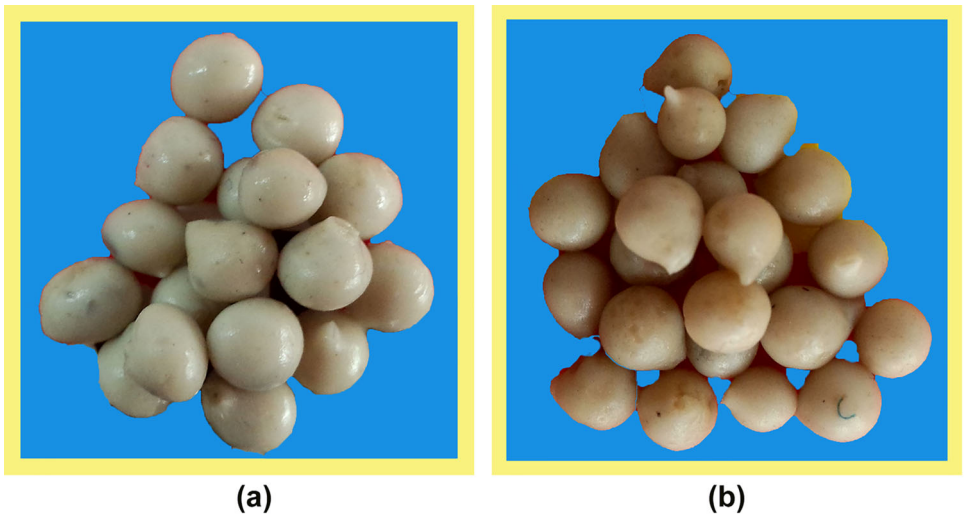

Fig. 10 The image of **a** PVA/2 wt% PPG hydrogel beads immobilized with microorganisms before aeration **b** PVA/2 wt% PPG hydrogel beads immobilized with microorganisms after aeration for 10 months

Effect of PPG on the Permeability and Swelling Behavior of PVA Gel Beads

The permeability of PVA gel beads by addition of different content of PPG was depicted in Fig. 11. It can be seen that UV transmission of ink solution at band 450–700 nm fluctuated slightly and reached up to over 90 % with different addition of PPG, implying that the high permeability of the gel beads can be kept well.

The swelling ratio of PVA hydrogel beads with varying content of PPG as a function of swelling time was shown in Fig. 12. It can be seen that in the initial swelling stage, all samples of gel beads absorbed water rapidly. The swelling ratio increased dramatically with time, and reached equilibrium in about 90 min. The swelling kinetics of PVA hydrogel beads was analyzed by assuming that the swelling process met the first order kinetic equation:

$$dQ_t/d_t = k(Q_e - Q_t) \tag{3.9}$$

where t was swelling time; Q_t, the swelling ratio at time t; Q_e, the equilibrium swelling ratio, dQ_t/d_t, the swelling rate; and k, the swelling rate constant. The swelling kinetics equation can be obtained by integral of the above equation:

$$Q_t = Q_e - (Q_e - Q_0)/e^{kt} \tag{3.10}$$

Another form of the equation can be written as:

$$kt = ln[(Q_e - Q_0)/(Q_e - Q_t)] \tag{3.11}$$

By plotting the graph of $ln[(Q_e - Q_0)/(Q_e - Q_t)]$ versus time t, as shown in Fig. 13, the swelling rate constant k can be obtained from the slope of the curve, which exhibited good linear relationship. The swelling rate constant k and equilibrium swelling rate of PVA hydrogel beads with varying content of PPG were listed in Table 4. It can be seen that with increasing content of PPG, the swelling rate

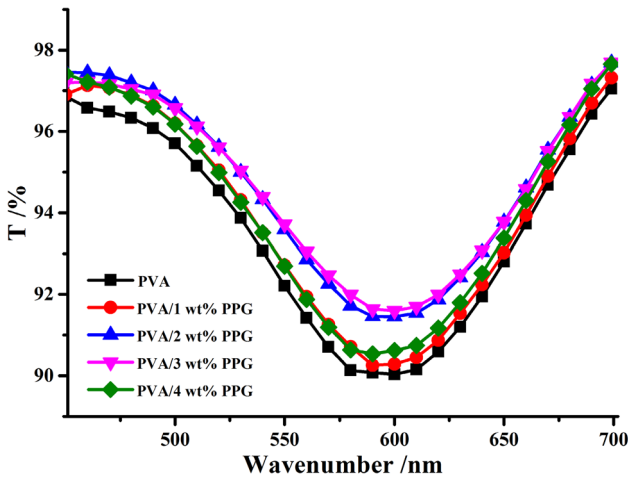

Fig. 11 UV spectrum of PVA hydrogel beads with various PPG content

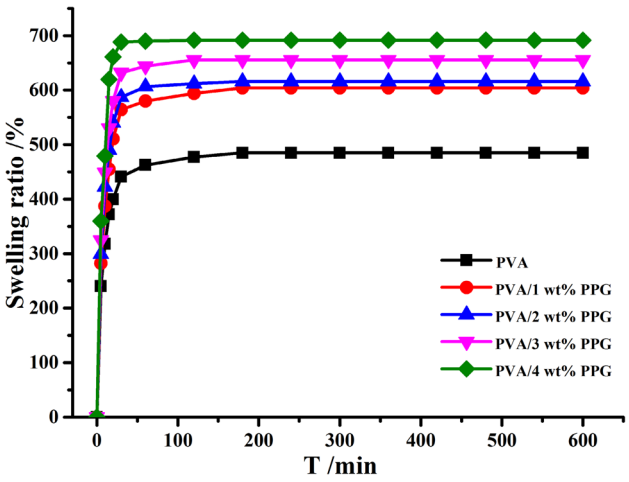

Fig. 12 The swelling ratio curve of PVA hydrogel with various PPG content

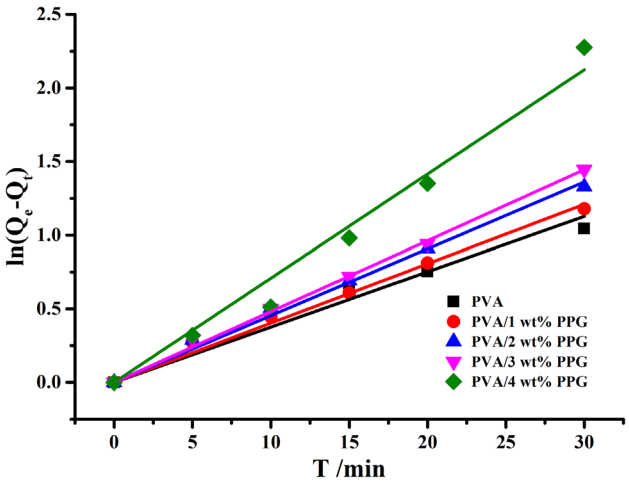

Fig. 13 The swelling kinetics of PVA hydrogel with various PPG content

constant k and the equilibrium swelling ratio of PVA gel beads increased, indicating that PPG could enhance the capillary water absorption capacity of PVA hydrogel. As shown in Fig. 14, after swelling, the porous structure of PVA/2 wt% PPG hydrogel remained well.

Effect of PPG on the Microbial Activity of PVA Hydrogel Immobilized with Microorganism

The PVA hydrogel immobilized with activated sludge was applied in waste water treatment. OUR was an important parameter to characterize the microbial activity of activated sludge in the waste water treatment process. The effect of PPG on DO variation with time of PVA hydrogel beads in the saturated aerated distilled water was depicted in Fig. 15. The value of OUR was calculated and listed in Table 5. It can be seen that DO values of varying samples

Table 4 The swelling rate constant of PVA hydrogel with various PPG content

Sample	Swelling rate constant k(h^{-1})	Equilibrium swelling ratio (%)
PVA	2.25	485
PVA/1 wt% PPG	2.42	604
PVA/2 wt% PPG	2.72	616
PVA/3 wt% PPG	2.89	655
PVA/4 wt% PPG	4.25	692

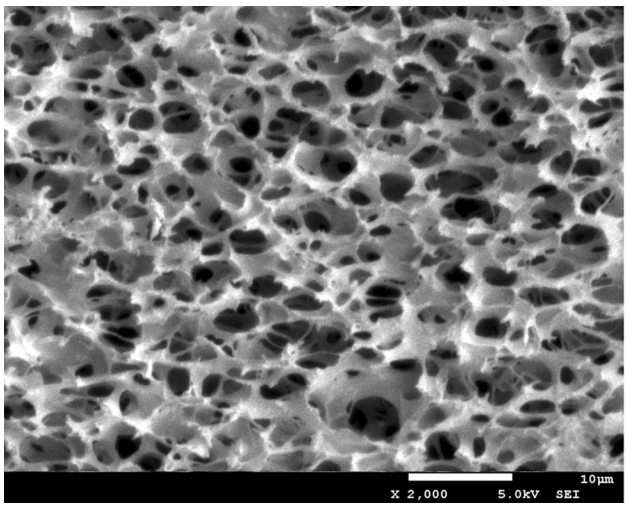

Fig. 14 SEM image of the cross section of the swelling PVA/2 wt% PPG hydrogel

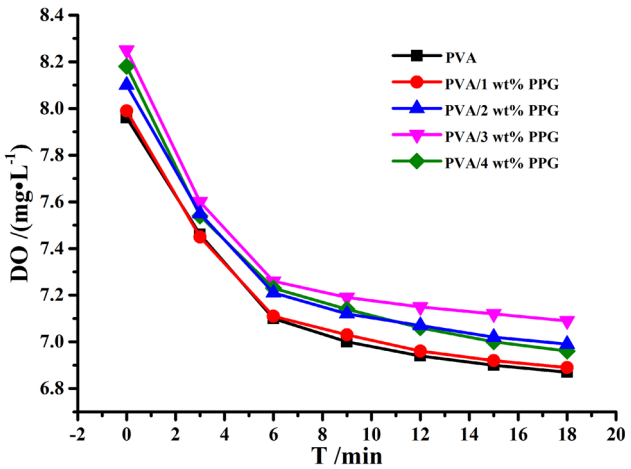

Fig. 15 DO-t curve of PVA hydrogel beads with various PPG content

of gel beads decreased with time, and the value of OUR slightly increased from 0.061 to 0.068 with increasing content of PPG.

The effect of PPG content on the COD removal rate of PVA hydrogel was investigated, as shown in Table 5. The COD removal rate of PVA hydrogel increased from 60 to 64 % with increasing content of PPG, implying that the formed uniform pores of PVA hydrogel beads were beneficial to supply channels for mass transfer of microorganism, and the microbial activity of the gel beads can be kept well. All the PVA hydrogel beads with porous structure had good permeability, providing channels for mass transfer, while the microbial reaction mainly controlled the waste water treatment efficiency. Therefore, the microbial activity and COD removal rate had no significant change by addition of PPG.

Conclusions

The toughening PVA hydrogel beads were prepared by incorporation of PPG through H_3BO_3-chemical crosslinking method. It was found that PPG could increase the consumption of H_3BO_3 and accelerate the crosslinking reaction of PVA. Thus the pore size of surface layer and core layer of PVA hydrogel beads can be controlled, and the porous structure became more uniform. With increasing PPG content, G' and ν_e increased first, reached maximum in presence of 2 wt% PPG, and decreased afterwards, indicating that a relatively low content of PPG could promote the formation of relatively uniform and dense network structure in PVA hydrogel, resulting in an improvement of tensile property and the hydraulic impact resistance of PVA hydrogel beads. PVA/2 wt% PPG immobilized with microorganism exhibited long-term hydraulic stability. The toughening mechanism of PPG on

Table 5 OUR and COD removal rate of PVA hydrogel with various PPG content

Sample	PVA	PVA/1 wt% PPG	PVA/2 wt% PPG	PVA/3 wt% PPG	PVA/4 wt% PPG
OUR (mg L^{-1} min^{-1})	0.061	0.061	0.064	0.062	0.068
COD removal rate (%)	60.44	60.55	61.54	63.01	64.46

PVA hydrogel was explored. By addition of PPG, the capillary water absorption capacity of PVA hydrogel can be enhanced and the high permeability can be kept well. More importantly, the value of the oxygen uptake rate (OUR) and COD removal rate of the PVA hydrogel immobilized with activated sludge had no obvious difference with addition of PPG, implying that a high microbial activity of the gel beads can be kept well.

Acknowledgments This work was financially supported by State Key Laboratory of Polymer Materials Engineering of China (Grant No. sklpme2016-2-07).

References

1. Leemen EJTM, Dos Santos VAP (1996) Characteristics of and selection criteria for support materials for cell immobilization in wastewater treatment. Water Res 30(12):2985–2996
2. Lebeau T, Robert JM (2006) Biotechnology of immobilized microalgae: a culture technique for the future? Algal Cult, Analog Blooms Appl 2:801–837
3. Mallick N (2003) Biotechnological potential of chlorella vulgaris for accumulation of Cu and Ni from single and binary metalsolutions. World J Microbiol Biotechnol 19:695–701
4. Michael ZC (1997) Hu, Mark Reeves. Biosorption of uranium by pseudomonas aeruginosa strain CSU immobilized in a novel matrix. Biotechnol Prog 13(1):60–70
5. Bauer A, Layh N, Syldatk C, Willetts A (1996) Polyvinyl alcohol immobilized whole-cell preparations for the biotransformation of nitriles. Biotechnol Lett 18(3):343–348
6. Covarrubias SA, Luz E (2012) Alginate beads provide a beneficial physical barrier against native microorganisms in wastewater treated with immobilized bacteria and microalgae. Appl Microbiol Biotechnol 93(6):2669–2680
7. Oh HS, Yeon KM (2012) Control of membrane biofouling in MBR for wastewater treatment by quorum quenching bacteria encapsulated in microporous membrane. Environ Sci Technol 46(9):4877–4884
8. Ting YP, Sun G (2000) Use of polyvinyl alcohol as a cell immobilization matrix for copper biosorption by yeast cells. J Chem Technol Biotechnol 75(7):541–546
9. Lozinsky VI, Plieva FM (1998) Poly (vinyl alcohol) cryogels employed as matrices for cell immobilization. 3. Overview of recent research and developments. Enzyme Microb Technol 23(3):227–242
10. El-Naas MH, Al-Muhtaseb SA (2009) Biodegradation of phenol by Pseudomonas putida immobilized in polyvinyl alcohol (PVA) gel. J Hazard Mater 164(2):720–725
11. Long Z, Huang Y (2004) Immobilization of Acidithiobacillus ferrooxidans by a PVA–boric acid method for ferrous sulphate oxidation. Process Biochem 39(12):2129–2133
12. Chang IS, Kim CI, Nam BU (2005) The influence of poly-vinyl-alcohol (PVA) characteristics on the physical stability of encapsulated immobilization media for advanced wastewater treatment. Process Biochem 40(9):3050–3054
13. Yujian W, Xiaojuan Y, Hongyu L (2006) Immobilization of Acidithiobacillus ferrooxidans with complex of PVA and sodium alginate. Polym Degrad Stab 91(10):2408–2414
14. Siripattanakul S, Wirojanagud W (2009) Atrazine removal in agricultural infiltrate by bioaugmented polyvinyl alcohol immobilized and free Agrobacterium radiobacter J14a: a sand column study. Chemosphere 74(2):308–313
15. Magrí A, Vanotti MB, Szögi AA (2012) Anammox sludge immobilized in polyvinyl alcohol (PVA) cryogel carriers. Bioresour Technol 114:231–240
16. Zhang Y, Ye L (2014) Structure and property of polyvinyl alcohol/precipitated silica composite hydrogels for microorganism immobilization. Compos B 56:749–755
17. Sirousazar M, Kokabi M, Hassan Z, Bahramian A (2012) Mineral kaolinite clay for preparation of nanocomposite hydrogels. J Appl Polym Sci 123(1):E122–E130
18. Li J, Suo Z, Vlassak JJ (2014) Stiff, strong, and tough hydrogels with good chemical stability. J Mater Chem B 2:6708–6713
19. Dave R, Madamwar D (2006) Esterification in organic solvents by lipase immobilized in polymer of PVA–alginate–boric acid. Process Biochem 41:951–955
20. Idris A, Zain NAM, Suhaimi MS (2008) Immobilization of Baker's yeast invertase in PVA–alginate matrix using innovative immobilization technique. Process Biochem 43:331–338
21. Jianlong W, Wenhua H, Yi Q (1995) Immobilization of microbial cells using polyvinyl alcohol (PVA)-polyacrylamide gels. Biotechnol Tech 9(3):203–208
22. Dave R, Madamwar D (2006) Immobilization of Acidithiobacillus ferrooxidans by a PVA–boric acid method for ferrous sulphate oxidation. Process Biochem 41:951–955
23. Kang HG, Lee SB, Lee YM (2004) Novel preparative method for porous hydrogels using overrun process. Polym Int 54(3): 537–543
24. Jiang X, Lu X, Xiao B, Wan Y, Zhao Y (2012) In vitro growth and activity of chondrocytes on three dimensional polycaprolactone/chitosan scaffolds. Polym Adv Technol 23(1):99–107
25. Surmacz-Gorska J, Gernaey K, Demuynck C, Vanrolleghem P, Verstraete W (1996) Nitrification monitoring in activated sludge by oxygen uptake rate (OUR) measurements. Water Res 30(5): 1228–1236
26. Van Hulle SW, Vandeweyer HJ, Meesschaert BD, Vanrolleghem PA, Dejans P, Dumoulin A (2010) Engineering aspects and practical application of autotrophic nitrogen removal from nitrogen rich streams. Chem Eng J 162(1):1–20
27. Masaru M, Yoshihiro U (1979) An application of ultraviolet spectrophotometric method for evaluation of organic matter in river water. Aichi-ken Kogai Chose Senta Shobo 7:54–59
28. Mrkva M (1983) Evaluation of correlations between absorbance at 254 nm and COD of river waters. Water Res 17(2):231–235
29. Colt J (2006) Water quality requirements for reuse systems. Aquac Eng 34(3):143–156
30. Annunziata L, Diallo AK, Fouquay S (2014) α, ω-Di (PPG carbonate) telechelic polyesters and polyolefins as precursors to polyhydroxyurethanes: an isocyanate-free approach. Green Chem 16(4):1947–1956
31. Gu J, Yang X, Lv Z, Li N, Liang C, Zhang Q (2016) Functionalized graphite nanoplatelets/epoxy resin nanocomposites with high thermal conductivity. Int J Heat and Mass Transfer 92:15–22
32. Gu J, Zhang Q, Tang Y (2008) Studies on the preparation and effect of the mechanical properties of titanate coupling reagent modified beta-Sic whisker filled celluloid nano-composites. Surf Coat Tech 202(13):2891–2896
33. Wang T, Turhan M, Gunasekaran S (2004) Selected properties of pH-sensitive, biodegradable chitosan–poly(vinyl alcohol) hydrogel. Polym Int 53(7):911–918
34. Wise ET, Weber SG (1995) A simple partitioning model for reversibly crosslinked polymers and application to the poly(vinyl alcohol)/borate system ("slime"). Macromolecules 28:8321–8327
35. Cencetti C, Bellini D, Pavesio A, Senigaglia D, Passariello C, Virga A, Matricardi P (2012) Preparation and characterization of antimicrobial wound dressings based on silver, gellan, PVA and borax. Carbohydr Polym 90:1362–1370